Journal of Solid State Chemistry 263 (2018) 24–29

Contents lists available at ScienceDirect

Journal of Solid State Chemistry

journal homepage: www.elsevier.com/locate/jssc

Y_2S_3 – Y_2O_3 phase diagram and the enthalpies of phase transitions

P.O. Andreev[a,*], L.A. Pimneva[b]

[a] University of Tyumen, 6 Volodarskogo St, 625003 Tyumen, Russia
[b] Federal State budget institution of higher education “Tyumen Industrial University”, 38 Volodarskogo St, 625000 Tyumen, Russia

ARTICLE INFO

Keywords:
Yttrium sulfide
Yttrium oxysulfide
Phase diagram
Thermal analysis
Melting enthalpy
Phase transformation

ABSTRACT

A phase diagram of the Y_2S_3-Y_2O_3, system has been defined from 1000 K to melts for the first time; the enthalpies of phase transitions in the systems have been determined. The monoclinic phase δ-Y_2S_3 ($P2_1/m$, a = 1.7523(8) nm, b = 0.4010(9) nm, c = 1.0170(7) nm, β = 98.60(6)°; microhardness H = 411 ± 7 HV) transforms at 1716 ± 7 K to the unquenchable high-temperature phase ξ-Y_2S_3, ΔH = 29 ± 6 J/g (7.9 KJ/mol) as determined by DSC. The quenching can't latch the Y_2S_3-phase. The melting point of Y_2S_3 is 1888 ± 7 K; ΔH = 150 ± 28 J/g (41.1 KJ/mol). Y_2OS_2 has a monoclinic structure (*P*21/*c*, a = 0.8256(8) nm, b = 0.6879(8) nm, c = 0.6848(8) nm, β = 99.52(6), H = 491 ± 13 HV) and melts incongruently at 1790 ± 8 K, ΔH = 190 ± 45 J/g (52 KJ/mol) by the scheme $Y_2OS_2 \leftrightarrow Y_2O_2S + L$ (16 mol% Y_2O_3). Y_2O_2S has a hexagonal structure (a = 0.3784(5) nm, c= 0.6584(4) nm, H = 654 ± 7 HV). Its congruent melting temperature is 2350 ± 40 K as determined by visual polythermal analysis (VPTA). The eutectic formed by Y_2S_3 and Y_2OS_2 phases has the composition 14.0 ± 0.5 mol% Y_2O_3 ($0.58Y_2S_3 + 0.42Y_2OS_2$) and melting temperature 1770 ± 6 K; ΔH = 215 ± 39 J/g. Between Y_2O_2S and Y_2O_3 phases, there is a eutectic with the coordinates 80 ± 1 mol% Y_2O_3 ($0.6Y_2O_2S + 0.4Y_2O_3$) and melting temperature 2150 ± 35 K (VPTA).

1. Introduction

Yttrium dioxosulfide Y_2O_2S ($1Y_2S_3$ $2Y_2O_3$), a member of Ln_2O_2S (Ln = La-Lu) family, is used as a matrix in crystal phosphor design [1,2]. The doped Y_2O_2S nanoparticles were prepared from electrospun poly(vinylpyrrolidone) composite using sulfur powder [3–5]. The morphology of Y_2O_3: Eu^{3+}; Y_2O_3: Yb^{3+}; Er^{3+} precursor particles was preserved during the synthesis. Yang et al. fabricated $Y_2O_3S:Eu^{3+}$ nanobelts 6.7 × 125 nm^2 in size and the phosphor possessed red emission peaks at 628 and 618 nm under excitation by 325-nm UV light [3]. Han et al. manufactured hollow $Y_2O_3:Eu^{3+}$ nanofibers with the outer diameter averaging 184 ± 26 nm that gave peaks in the red at 628 and 618 nm under excitation by 260-nm UV light [4]. The optimal Eu^{3+} concentration was 3 mol%. Lu et al. fabricated $Y_2O_2S:Yb^{3+}$, Er^{3+} nanofibers having the diameter 105 ± 13 nm using polyvinylpyrrolidone. The nanofibers showed strong green and red emission under excitation at 526, 548, and 668 nm, respectively [5].

The Ce^{3+} doped $Y_2O_2S:Er^{3+}$ luminophore can be used to suppress the visible anti-Stokes luminescence when excited in the range 0.90–0.98 μm [6]. The $(Y_{1-x}\,Er_x)_2O_2S$ solid solutions were found to luminesce in the range 400–2000 nm under excitation with 790- and 810-nm laser beams [7]. The $(Y_{1-x}Eu_x)_2O_2S$ solid solution shows emission in the range 450–1600 nm under 365- nm excitation [8]. In the $Y_{1.80}Er_{0.10}Yb_{0.10}$ O_2S phosphor, visible luminescence was observed when two resonance infrared photons of different energies were absorbed successively [9]. Complex yttrium oxide compounds, whose structures are related to the Y_2O_2S structure, have been studied as optical materials and solid electrolytes [10,11]. The Y_2O_2S:Eu has lower density compared to Gd_2O_2S:Eu [12,13], which allows to consider them as promising biomarkers for living systems. Y_2S_3/ZnO nanocomposites are efficient photocatalysts for decomposition of organic compounds [14]. In an aqueous phase at pH 7, the Y_2S_3 in the composite should partially hydrolyze to yield yttrium oxysulfides. Nanocrystalline Y_2O_3:Eu samples are promising light-emitting-diode materials [15]. Luminescence is also typical of salt compounds of yttrium [16].

The extensive studies of Y_2O_2S-based materials and their practical importance make it topical to investigate the Y_2S_3-Y_2O_3 phase diagram, which will serve as the scientific base of further investigations. Two compounds are formed in the Y_2S_3-Y_2O_3 system: hexagonal Y_2O_2S, space group $P\bar{3}ml$, a = 0.3789 nm, c = 0.6588 nm [17]; and monoclinic Y_2OS_2 ($2Y_2S_3$ $\cdot 1Y_2O_3$), space group *P*21/*c*, a = 0.8255 nm, b = 0.6885 nm, c = 0.6853 nm, β = 99,63°, z = 4 [18]. “Faint yellow brick-shaped single crystals of Y_2OS_2 were produced as a by-product of oxidizing $YClH_{0.67}$ (or $Na_{0.25}YClH_{0.75}$) by sulfur in a tantalum ampoule at 1123 K for 7 days when oxygen-contaminated starting chlorides (e.g., YOCl) were used [18].”

There have been no intentional studies of Y_2S_3-Y_2O_3 phase diagram

---

[*] Corresponding author.

https://doi.org/10.1016/j.jssc.2018.03.001
Received 25 October 2017; Received in revised form 1 March 2018; Accepted 4 March 2018

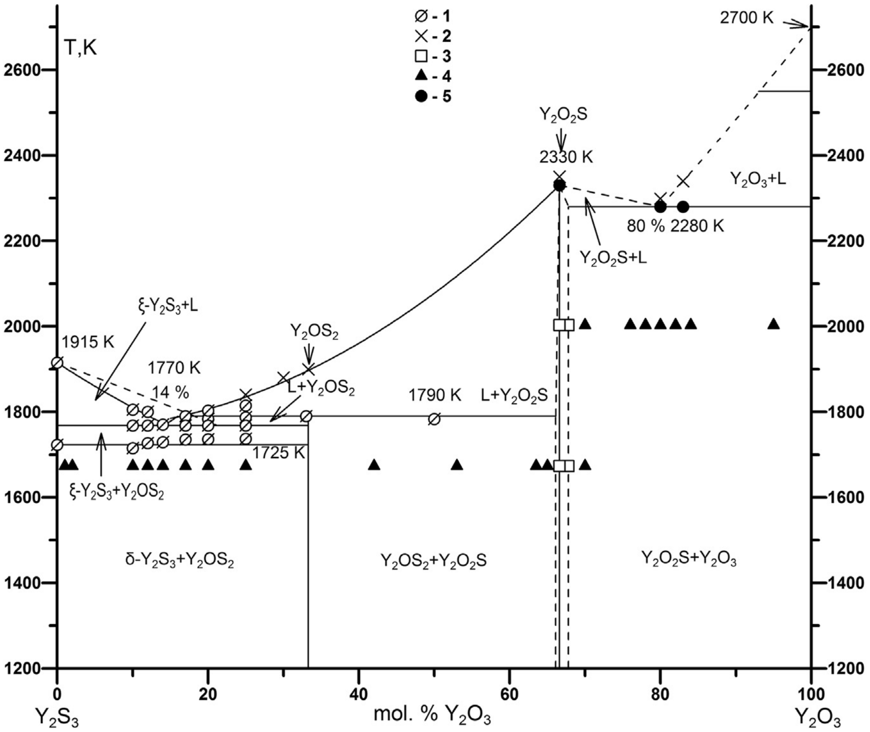

Fig. 1. Phase diagram of the Y_2S_3 - Y_2O_3 system: 1 - complete sample melting; 5 - initiation of sample melting. The state of the samples according to physicochemical data: 2 - single phase: 4 - two phases mixture. DTA/DSC data: 3 - liquidus line temperatures.

as yet. The boundaries of Y_2O_2S-base solid solutions in the Y_2S_3-Y_2O_3 system, the thermal stability of Y_2O_2S and Y_2OS_2, and their melting characters and temperatures were not elucidated. The phase transition enthalpy values can be used to calculate the liquidus lines by the Schroeder equation from the melting temperatures and enthalpies [19].

Sesquisulfide δ-Y_2S_3 crystallizes in monoclinic space group $P2_1/m$ with a = 1.7523 nm, b = 0.4010 nm, c = 1.0173 nm, β = 98.60o, z = 6 [18,20,21] and melts congruently at 2010 K [19,21]. Y_2O_3 has a cubic structure of space group Ia3, a = 1.061 nm, z = 16; it transforms to a hexagonal phase (space group P3m1, a = 0.381 nm, c = 0.609 nm, z = 1) at 2550 K; and melts congruently at 2680 K [22].

Thus, the present study is aimed at the exploration of the phase diagram of Y_2S_3-Y_2O_3 system and determination of enthalpy values for the phase transitions found in the system.

2. Experimental

Monoclinic δ-Y_2S_3 was prepared in the powder by exposing Y_2O_3 (Russia, 99,98 mol% Y_2O_3) to an H_2S + CS_2 flow at 1270–1370 K [23,24]. Gaseous CS_2 and H_2S were prepared by thermal decomposition of NH_4CNS (Russia, 99 mol% NH_4CNS) [25]. The phase transition sequence was observed to be $Y_2O_3 \rightarrow Y_2O_2S \rightarrow$ δ-Y_2S_3. The phase constitution of samples was monitored by microstructural analysis (MSA) and X-ray powder diffraction. The presence of even individual Y_2OS_2 crystals in δ-Y_2S_3 was detected by microstructural analysis of sintered or cast samples. We prepared single-phase δ-Y_2S_3 powders with a = 1.7523(8) nm, b = 0.4010(9) nm, c = 1.0173(7) nm, β = 98,60(6)°, which correlates with [18].

Y_2O_2S was prepared in the single-phase powder by consecutively exposing $Y_2(SO_4)_3$ (Russia, 99.98 mol% $Y_2(SO_4)_3$) first to an H_2 flow at 770–870 K for 4 h and then to an H_2S flow at 1170–1220 K for 5 h [26].

The Y_2S_3-Y_2O_3 samples containing 0–60 mol% Y_2O_3 were prepared by alloying Y_2S_3 and Y_2O_2S precursors in graphite crucibles. The 60–100 mol% Y_2O_3 samples were alloyed and annealed in tantalum crucibles. The crucibles were mounted in a silica glass reactor, which was equipped with Al_2O_3 thermal screens. The reactor was pre-evacuated and then filled with Ar (99.998%, Russia) to create an excessive pressure of up to 10 Pa. The thus-prepared cast or sintered samples were then annealed at 1770 K for 0.7–1 h (0–60 mol% Y_2O_3 samples) and for 1 h (60–95 mol% Y_2O_3 samples). When annealed at 1070° C for up to 3000 h, samples were placed in evacuated and sealed-off silica glass ampoules.

Differential scanning calorimetry (DSC) and thermogravimetric analysis (TG) was performed on a STA 449 F3 Jupiter instrument equipped with a W 3%Re - W 25% Re thermocouple in He (99.99999%, Russia) flow (30 ml. per. min.). Sample sizes were 98–103 mg, with the accuracy of an integrated balance equal to ± 0.01 mg. The temperature adjustment accuracy was 0.3 K; the heating rate in the ranges where thermal events were observed was 5 K/min. The results of STA experiments were processed in the Proteus-6 program package. The precision in the phase transition enthalpy determination was ± 18%. In visual polythermal analysis (VPTA), a 40–50 mg sample was placed in a tantalum crucible, which was then mounted on a W 5%Re - W 35% Re thermocouple. VPTA experiments were carried out under argon atmosphere (99.998%); the heating rate was 15–30 K/min. The references used were SrF_2 (T = 1750 K), Pt (T = 2033 K), Cr (T = 2180 K), and Al_2O_3 (T = 2326 K) [27,28].

X-ray powder diffraction patterns were recorded on a DRON-7 using CuKα radiation. Unit cell parameters were calculated in the PDWin-4 program. Microstructures were observed on polished samples using an AxioVert. A1MAT microscope (the AxioVision SE64 program). Microhardness was measured on an HMV-G21DT tester (NaCl reference, H = 791 HV) under the load 490.4 mN. The chemical composition of grains in samples and grain images were determined using a Jeol 6510 LV scanning electron microscope equipped with an energy-dispersive spectrometric unit [29,30].

3. Results and discussion

We are the first to plot the Y_2S_3-Y_2O_3 phase diagram (Fig. 1), to